Facade Solar Potential Analysis: Empirical Assessment and Geospatial Visualization for Bahrain's High-Rise building

Ryali, D.,* **Jalal, F. and Gollapudi, L. N.**
Faculty of Engineering, Bahrain Polytechnic, Kingdom of Bahrain
E-mail: divya.ryali@polytechnic.bh
**Corresponding Author*

DOI: https://doi.org/10.52939/ijg.v22i5.4978

Abstract
Bahrain is currently facing significant energy demand due to rapid urbanization and a growing population, with power usage exponentially increasing, leading to increased carbon emissions. In response, the Bahrain government is exploring renewable energy options such as waste-to-energy, wind, and solar power. Bahrain targets solar PV of 400 MW by 2035. Solar energy plays a vital role in addressing environmental concerns and reducing reliance on conventional energy sources. Its integration into urban settings is essential for meeting rising energy demands and achieving sustainable development goals. The research assesses the solar potential of a selected tall building -United Tower in Bahrain using a comprehensive geospatial analysis with ANSYS Fluent and the Ghouard's Solar Model. Primary data for constructing a virtual 3D model was sourced from Google Earth. The study evaluates the building's design and orientation to determine its solar energy potential and classification as a green building. The key focus is the analysis of solar potential on all surfaces, particularly vertical facades. Solar distribution was examined at five intervals throughout the day to capture the dynamic solar exposure. Empirical modeling based on the Ghouard's Solar Model was employed to assess the building's response to solar radiation, followed by a comparative study between the empirical results and ANSYS Fluent simulations. During the summer solstice, peak solar potential was observed at mid-day, with ANSYS FLUENT recording 780.25 W/m² and Ghouard's Model 790.89 W/m². In contrast, the winter solstice showed the lowest potential, at 284.75 W/m² for method-1 and 289.24 W/m² for method-2. Findings indicate that the tall building can harness substantial solar energy, contributing positively to Bahrain's renewable energy objectives.

Keywords: Geospatial Visualization, Geospatial Analysis, Solar Potential

1. Introduction

Bahrain's national plan aims for 20% renewable capacity by 2035, primarily through solar PV, as part of its SDG and climate targets. These ambitions are explicitly linked to SDGs such as Affordable and Clean Energy (SDG 7) and Climate Action (SDG 13) [1]. These targets contribute to carbon emission reduction, water conservation, and job creation, and key SDG outcomes. The GCC has historically depended on fossil fuels to fulfill its energy needs due to abundant oil and gas reserves. However, there is a growing recognition of the necessity to diversify the energy mix, reduce fossil fuel consumption, and limit greenhouse gas emissions. This shift aims to enhance sustainability in buildings by lowering energy use and integrating renewable energy sources. In the GCC region, particularly in Saudi Arabia, the focus has been on large utility-scale photovoltaic (PV) projects rather than building-applied PV (BAPV) systems. The building sector in Gulf region is rapidly expanding and is significant in terms of energy consumption and carbon emissions [2]. Over the past decade, GCC countries have actively promoted sustainable urban development and energy efficiency through various policies and legislative measures. This commitment has facilitated the rapid adoption of sustainable technologies and renewable energy solutions to address environmental challenges, with solar and wind power as key clean energy sources. However, progress in the broader GCC (Gulf Cooperation Council) is generally behind schedule, revealing a gap in achieving the full range of SDG indicators by 2030 unless further action is taken [2][3]. Bahrain, as a small island nation in the Arabian Gulf, faces significant challenges related to

limited land availability, rapid urbanization, and high energy demands. These factors make traditional ground-mounted solar farms less feasible [4]. Studies indicate that for solar PV projects, land use, environmental trade-offs, and social acceptance must be carefully managed, especially in dense or resource-poor regions [5]. The efficiency of land occupation by solar projects becomes crucial, innovative approaches like building-integrated PV (BIPV), floating PV on reservoirs, and agrivoltaics (dual-use with agriculture) are gaining attention globally and starting to be discussed in the Gulf context [6].

A study revealed that most buildings in Bahrain lack sustainability features and inadequate environmental considerations, contributing to an energy crisis that accounts for about 80% of total electricity consumption. There is a scarcity of research on the implementation of photovoltaic (PV) systems in Bahrain's building sector. Assessing the integration of PV on building surfaces, particularly the walls of high-rise structures, is crucial for policymakers, government officials, and users. This research aims to fill that information gap [7].

Building-integrated photovoltaics (BIPV) where photovoltaic (PV) systems are part of the building envelope, particularly facades are an increasingly attractive option for harnessing solar energy in dense urban environments like Manama, Bahrain. Due to scarcity of open land, maximizing the potential of existing urban structures is critical in Bahrain. BIPV allows buildings to serve dual purposes: shelter and energy generation. Facade installations can capture substantial solar energy since Bahrain has high solar irradiance year-round. Case studies from Manama confirm the strategic importance of solar integration in buildings, with reports suggesting that solar technologies, when integrated into the building envelope involving walls/ facades, can meet a considerable portion up to 83% of a building's electricity demand under optimal conditions [7].

Recent advancements in BIPV technology have made facade-based PV systems more efficient and desirable. Research highlights innovations such as semi-transparent PV modules for windows, thin-film PV, and new mounting techniques that enhance system performance while meeting urban design and shading requirements. These solutions address unique urban challenges, including space constraints and architectural integration, by allowing PV to blend seamlessly with building aesthetics and existing urban infrastructure [9]. Bahrain's geographic location provides consistently high solar insolation, making facades which can be oriented to capture morning or afternoon sunlight promising for solar power generation [10]. While south-facing facades receive the maximum solar exposure, even east and west orientations in Bahrain yield significant output due to the region's intense sun. Studies reviewing urban solar integration in comparable climates demonstrate that facade PV can substantially contribute to onsite renewable generation in high-density urban centers [11].

Solar integration, particularly with BIPV, provides several co-benefits, including reduced urban heat island effects, lower greenhouse gas emissions, and improved urban resilience against climate change [12]. By combining PV with nature-based solutions (e.g., green walls), buildings can further enhance climate adaptation in hot climates like Bahrain's. The lessons from Bahrain echo trends observed in other arid and land-scarce countries across the Middle East and globally. Increasingly, solar on facades forms an essential part of reaching net-zero and climate neutrality goals in urban environments, as shown in studies from Europe and other Gulf States [13].

2. Solar Analysis on Facades

Solar façades are classified into two classes as opaque and transparent/semi-transparent categories [14]. This classification enhances the understanding of their varied applications and advantages in contemporary architecture. The author advocates for further research to optimize the performance of semi-transparent systems and smart windows, emphasizing the significance of solar façades in advancing sustainable building practices. Solar façades is a multifunctional element integrating renewable energy technologies [15]. It highlights the need for a deeper understanding of the aesthetic, technical, and functional challenges of building-integrated photovoltaics (BIPV). However, it has noted a gap in research regarding the long-term performance and economic viability of solar façades across various climates, emphasizing the need for empirical studies on durability and maintenance, particularly in standard buildings.

Polo's study focuses on modelling photovoltaic (PV) energy generation on building façades at the CIEMAT headquarters in Madrid. Utilizing satellite-derived solar data and high-resolution digital surface models, the study estimates PV generation for five arrays. While the south and west facades showed good accuracy, the east façade faced challenges due to shading from nearby trees. The research underscores the importance of detailed shadow modelling and suggests future studies incorporate dynamic modelling and long-term monitoring for improved PV assessments as cited in [16]. Putra et al. [17] examined vertical solar irradiance in Tangerang, Indonesia, using data from six pyranometer sensors.

The study highlighted the significance of east and west façades in receiving solar energy, especially during peak sunlight hours, illustrating their importance in green building design.

The impact of urban morphology on facade solar potential in Adelaide, Australia was investigated. The research found that south-facing façades received the highest solar radiation, while north façades received substantially less. The analysis indicated that solar potential varies with urban morphology, with low-density blocks showing the greatest energy harvesting potential [18]. A Trigonometric model (TgM) was introduced to improve solar irradiation predictions on building façades in urban Canada. The study revealed that south-facing façades achieved an average solar irradiation of 79.5 W/m², though narrower street configurations limited solar access significantly. East and west façades performed better in dense urban areas, benefiting from morning and evening solar exposure [19].

The study "Unleashing the green potential: Assessing Hong Kong's building solar PV capacity" analyses the solar potential of BIPV on facades and roofs in Hong Kong. Findings indicate façades have a substantial solar potential of approximately 2.48×10^{11} kWh, with south-facing façades receiving the most radiation. The research suggests that integrating BIPV systems could meet up to 16.32% of the city's electricity demand, highlighting the need for further studies on the economic implications of BIPV integration and the impact of urban shading on solar energy capture [20]. A study conducted by Divya and her colleagues investigated the solar potential of buildings in Jamshedpur, India, utilizing UAVs. The research revealed significant findings regarding the feasibility of solar energy generation in urban settings, highlighting that the orientation and design of buildings greatly influence solar efficiency. The study found that rooftops and vertical walls could collectively generate substantial energy, suggesting that integrating solar panels on both surfaces could maximize energy gain. Furthermore, the research emphasized the importance of local climate conditions and urban density in determining solar potential, providing valuable insights for future urban planning and sustainable architecture in similar regions [21].

The literature review shows the critical importance of solar analysis on building facades/walls, particularly in urban contexts where land is scarce. Given that building walls represent significant surface areas, they offer substantial potential for harnessing solar energy, thereby contributing to sustainable development. However, the current literature reveals a notable deficiency in studies focusing on solar analysis for building facades in the Kingdom of Bahrain. The need for comprehensive assessments to evaluate the solar potential of buildings before the installation of solar energy systems is essential. The research aims to address this gap by modelling a building in Bahrain, a small country with limited land and a notable presence of skyscrapers. The context presents a unique opportunity to examine how tall buildings can respond to solar energy potential. The selected building will be analysed to determine its capability to function as a green building based on solar energy utilization.

3. Study Area

The building chosen for this study is in the Kingdom of Bahrain. This area presents unique architectural and energy efficiency characteristics. In Figure 1, the exact location of the building within the Kingdom is highlighted, providing essential context for this research.

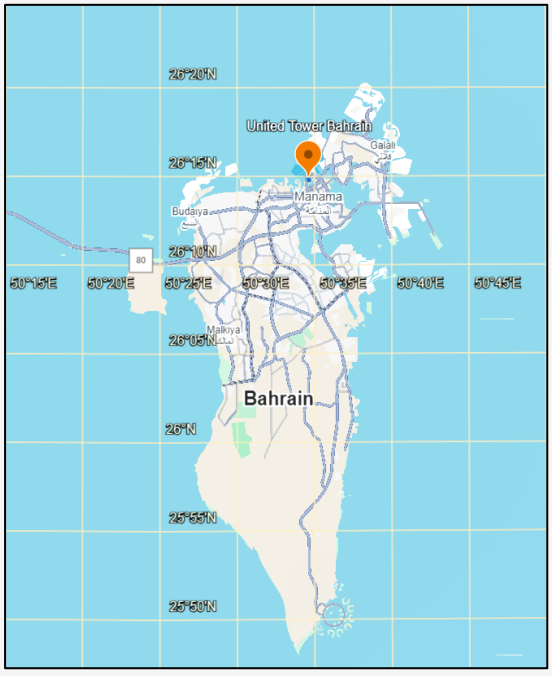

Figure 1: Kingdom of Bahrain

The United Tower was designed to be a multipurpose structure that would serve as a vertical spiral city. It features an unhindered 360-degree view of the Kingdom of Bahrain as shown in Figure 2. This building has been chosen due to its status as one of the tallest structures in the developing region. Additionally, the entire outer facade can be optimized for Building-Integrated Photovoltaics (BIPV), provided that the solar potential is viable. The tower has gained recognition as an iconic

"TwistScraper" due to its distinctive architectural design.

Figure 2: United Tower, the Kingdom of Bahrain

United Tower has been selected to conduct a 3D spatial analysis to estimate its solar potential. This research aims to assess the building's suitability for Building-Integrated Photovoltaics (BIPV) technology by simulating solar flux and visualizing the distribution of solar energy across its surfaces. By evaluating the solar potential of this iconic structure, the study underscores its capability to harness solar energy, contributing to sustainable building practices. The findings will enhance understanding of how tall architectural designs in the region can effectively capture solar energy, promoting sustainability in urban architecture. Google Earth and its Geometry Tools are used to collect geospatial data related to the location, area, building orientation, and perimeter of the tower. The latitude and longitude coordinates obtained are $26^{0}14'48''$ N and $50^{0}34'37''$ E respectively which are essential for constructing solar path as shown in Figure 3. As the coordinates are taken the geometry from Google Earth, there may be slight inconsistencies. However, these variations are unlikely to significantly impact the results of the solar potential analysis.

Additionally, data as per the Council on Tall Buildings and Urban Habitat (CTBUH), which ranks the United Tower as the 3003rd tallest building in the world, with a verified height of 189.2 meters and a floor area of 1,300 square meters. The dimensions, area, and perimeter derived from Google Earth are consistent with the information provided by CTBUH, establishing these dimensions as critical parameters for our modeling. Furthermore, the tower is managed by CBRE MENA, a global leader in commercial real estate services. Their promotional materials confirm that each floor of the tower offers an area of approximately 1,300 square meters, which aligns closely with our Google Earth findings. This approach to utilizing open-source data is cost effective and promising optimal research outcomes.

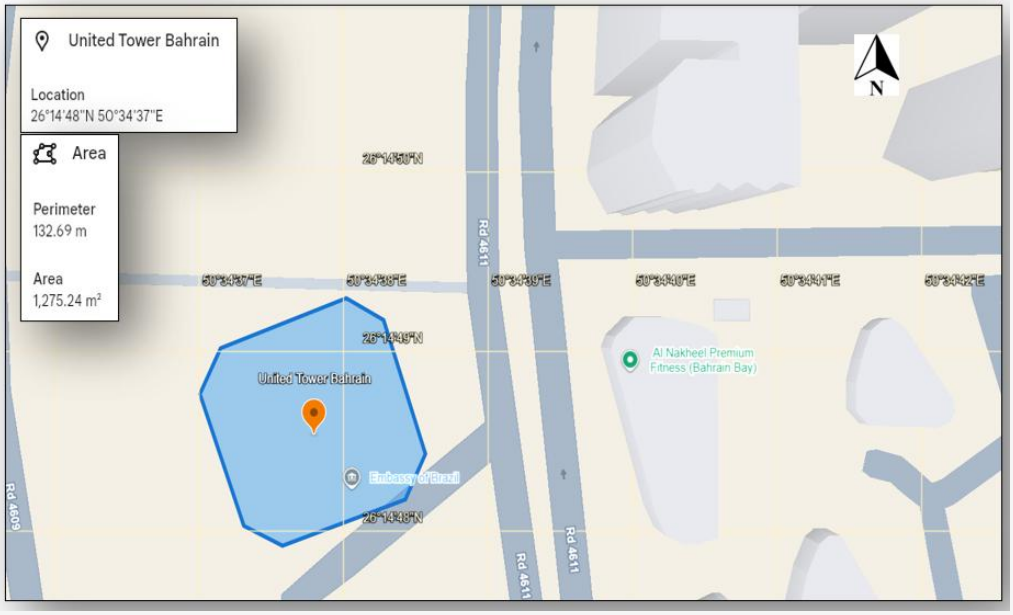

Figure 3: Geospatial information of Tower from google earth

4. Methodology

The study employs a comprehensive methodology for assessing solar potential, integrating engineering tools with empirical modeling techniques. Initially, the geographical location of the study area is determined using Google Earth, which provides precise latitude and longitude coordinates crucial for subsequent analyses [22]. Data collection is a critical phase, focusing on both spatial data and building geometries. Data concerning building height, dimensions are sourced from the Council of Tall Buildings and Urban Habitat. Details of building location, footprint area, orientation are from Google Earth [23]. Furthermore, SolidWorks is utilized to model three-dimensional representations of building, enhancing visualization and enabling the simulation of solar exposure on building facades along with rooftop throughout different times of the year [24].

The next step involved geospatial 3D simulations, executed using software ANSYS, which facilitated detailed modeling of the solar potential across the analyzed building surface areas. Numerous studies have effectively employed ANSYS for comprehensive solar analysis, leveraging its advanced simulation capabilities to evaluate solar energy potential in various contexts. By utilizing ANSYS, researchers can model complex geometries and accurately simulate the interactions between solar radiation and built environments. This allows for detailed assessments of factors such as shading, solar exposure, and thermal performance. ANSYS versatility in handling diverse scenarios ranging from urban landscapes to large-scale solar installations has made it a preferred tool in the field [25] and [26]. The sequential workflow is straightforward process as shown in Figure 4. For validation, solar potential analysis is carried using empirical model- Ghouard's Model to calculate Direct Irradiation, Diffuse Irradiation and Global Irradiation that incorporate the Turbidity factor and sky view factor. The sun path analysis is performed for calculating solar elevation and azimuth angles using Ghouard's Model, ensuring accurate representation of solar trajectories throughout the year [27]. This research focuses on simulating the solar potential of building walls of a selected building, Table 1 highlights the importance of this research by outlining key factors that contribute to the viability and effectiveness of solar investigations on building walls.

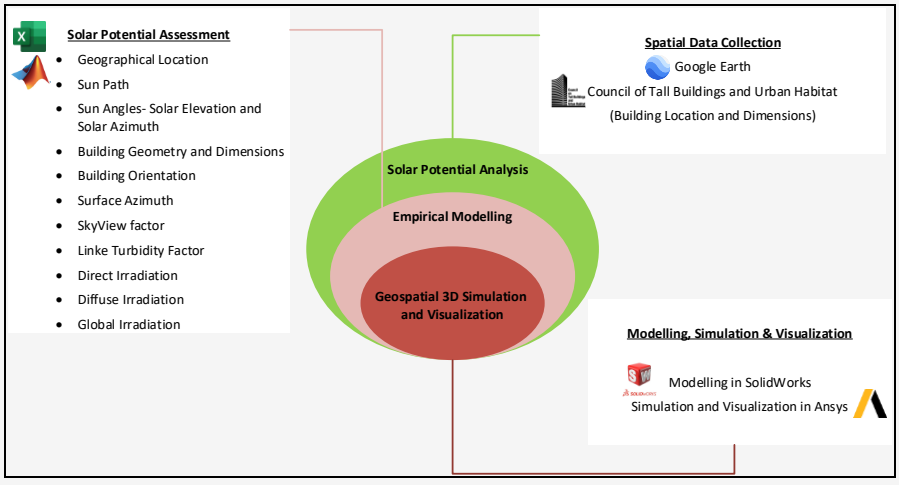

Figure 4: Schematic workflow for solar potential assessment

Table 1: Key points for BIPV facade potential in Bahrain

Dimension	Key Insights & Relevance
Land Limitation	Directs solar strategy toward vertical (facade) installations
Solar Potential	High year-round irradiance supports significant power yields even on non-south-facing facades
Efficiency Advancements	BIPV tech (semi-transparent PV, thin film) boosts effectiveness on varied facade architectures
Economic Incentives	Policy support (e.g., 30% subsidies) crucial for market uptake
Urban Challenges	Integration addresses shading, aesthetics, space via design innovations
Digital Management	AI and Digital Twins optimize energy capture and O&M
Environmental Impact	Contributes to decarbonization and climate adaptation as part of net-zero urban strategies
Regional Applicability	Findings align with best practices in MENA and global urban centres

5. Modelling

SolidWorks 2021 was used to generate an accurate life-sized model. As per the research, the building was 189.2m tall and had a base area of approximately 1273 m^2. The geometry was created by flex twisting the 4 corner rectangular offsets by 180 degrees. The figure showcased the flex feature used to achieve the desired twist for the building model as shown in Figure 5. The building model is shown in Figure 6. For further analysis, a rectangular enclosure was created from which the building volume was subtracted to create a cavity.

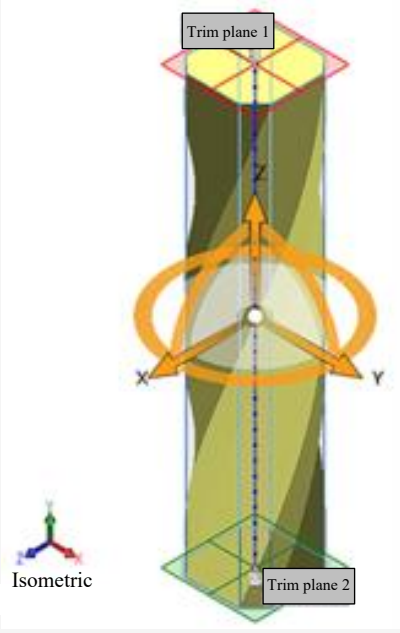

Figure 5: Using flex feature to achieve desired twist

Figure 6: Finalised building model

It is highly important to know that the enclosure size shouldn't be too small (prevents capturing accurate results) or large (computation time and error propagation increases). The enclosure creation for the analysis is shown the Figure 7.

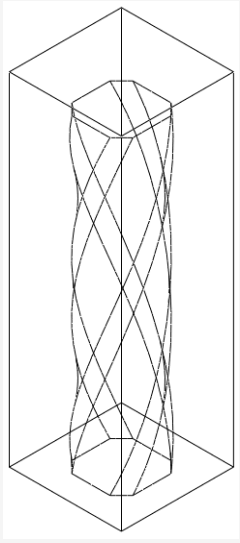

Figure 7: Enclosure creation for CFD analysis

6. ANSYS-Fluent Environment Setup

The CAD file was saved with a Parasolid extension and was imported into Ansys Fluent 2020 as shown in Figure 8. The 'DesignModeler' tool was used to check for any geometrical discontinuities and import errors.

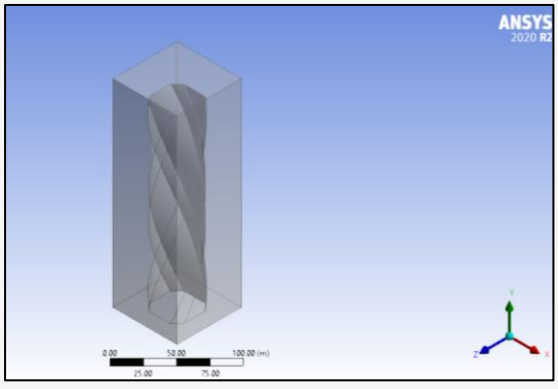

Figure 8: Importing CAD model in design modeler

Up next, the model's data was transferred to Meshing tool. Here, the named selections were made, highlighting the physical nature and properties of every surface: Inlet, Outlet, Side Free-Boundaries and the internal cavity joined with the floor wall acting as the base. The mesh views associated with this study can be observed in the figures provided. Figure 9 presents the external mesh view, while Figure 10 illustrates the internal mesh view.

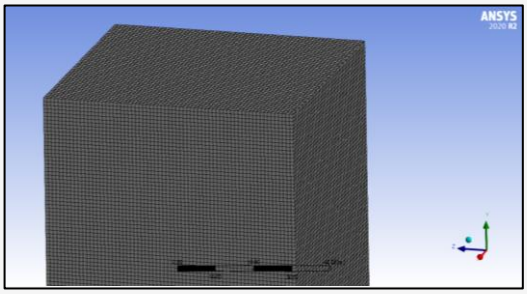

Figure 9: Final Mesh (Exterior view)

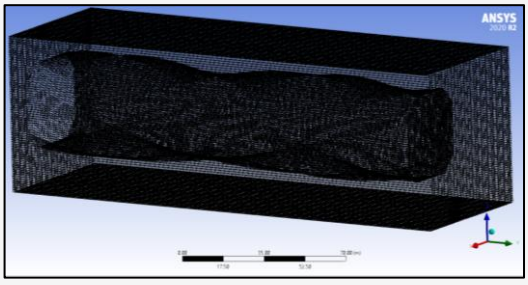

Figure 10: Final Mesh (Through View)

These visual representations are essential for understanding the structural design and spatial configuration of the building. For pre-meshing parameters, element size of 1m was selected and 'hex-dominant' method preference was applied. The final mesh had 765,038 nodes. Fluent setup was launched with 4 CPUs (Ryzen 5 4000 Series Processor), 1 GPU (Nvidia GTX 1650 Ti) and Double Precision method. Setting up the Fluent environment involved several configurations as shown in Table 2. The Rosseland radiation model was chosen to simulate radiative heat transfer through participating media, such as air within the enclosure. This model assumes the medium is optically thick and temperature gradients are relatively small, making it suitable for low-temperature, semi-transparent glass environments like solar-heated buildings. The glass façades in United Tower absorb and re-emit radiation, and while the dominant heat transfer mode is surface-based, radiation through the air still contributes to the overall thermal profile.

Table 2: Fluent setup

Criteria	Description
Solver Type	Pressure-Based
Velocity Formulation	Absolute
Time	Steady
Gravity	Disabled
Models:	Energy Equation Enabled
	Laminar Viscous Model
	Rosseland Radiation Model
Solar Load	Solar Ray Tracing
Sun Direction Vector	Governed by Solar Calculator
Direct Solar Irradiation	Governed by Solar Calculator
Diffuse Solar Irradiation	200 W/m^2 (Constant)
Spectral Fraction	0.5
Materials	Fluid: Air
	Solid: Glass-Soda-Lime-Common Glass
Inlet Face Boundary Conditions	Inlet Velocity: 3 m/s
	Outlet Gauge Pressure: 0
	Temperature: 300 K
	Radiation: Enabled
	Solar Transmissivity Factor: 1
Outlet Boundary Conditions	Gauge Pressure: 0
	Radiation: Disabled
Enclosure's Surface Boundary Conditions	Boundary Condition Type: Semi-Transparent
	Wall Motion: Stationary Wall
	Material: Air
	Radiation: Enabled
	Absorptivity Coefficients: 0
	Transmissivity Coefficients: 1
Building's Wall Boundary Conditions	Boundary Condition Type: Opaque
	Wall Motion: Stationary Wall
	Material: Common-Soda-Lime-Glass
	Radiation: Enabled
	Direct Visible Light Absorptivity: 0.8
	Direct IR Absorptivity: 0.8
Solution Methods	Pressure-Velocity Coupling: Coupled
	Gradient, Pressure, Momentum and Energy Discretisation: Second Order Upwind
Initialisation Method	Hybrid Initialisation
Iterations	500 (Maximum-Each Case)

Rosseland's model captures radiation diffusion within the enclosure, complementing surface absorption effects. The Solar Ray Tracing model is used to accurately compute direct beam solar radiation on the building's surfaces. It tracks individual rays from the sun as they interact with the geometry, enabling the simulation to account for: Time-of-day and date-specific sun position, Building orientation and surface angle and obstructions. This model allows high-fidelity simulation of irradiance variation by façade (East/West/South/North), which was critical for evaluating the PV integration potential. It gave precise surface heat flux values at different hours, matching the Excel model.

The Sun Direction Vector, governed by the Solar Calculator in Fluent, ensures that the incident angle and solar position change appropriately with the chosen date, time, and geographical coordinates (Bahrain). It removes manual guesswork from solar input. The sun's azimuth and elevation were auto calculated for needed date and time, resulting in realistic solar heating profiles without the need for approximations. The solar heat flux is simulated for equinox, summer and winter solstice. The simulation was carried out for the solar radiation received at different times throughout the day. The focus of analysis was on five times: 8:00 AM, 10:00 AM, 12 Noon 2:00 PM, and 6:00 PM. By capturing data at these intervals, aiming to highlight the fluctuations in solar heat flux and better understand the impact of solar positioning on energy potential. The Figures 11-13 display the simulates results on three key dates: March 21, June 21, and December 21. Each date showcases the performance across five defined intervals, illustrating variations in energy capture and efficiency throughout the year.

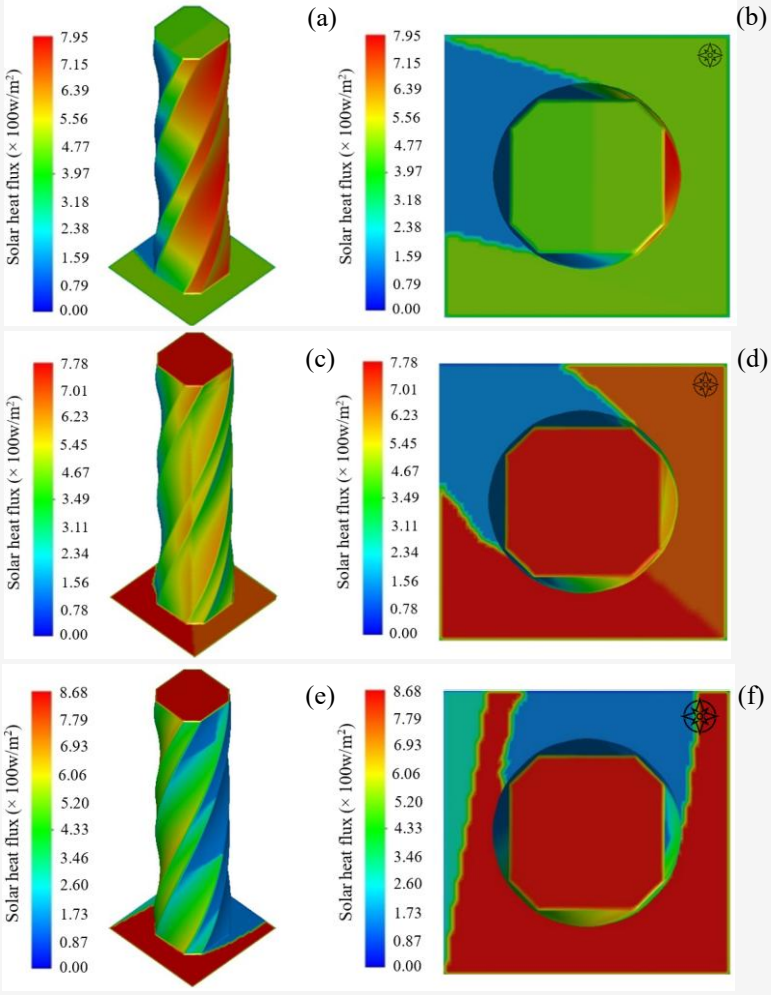

Figure 11: Simulation for March 21st, 2025
(a) isometric view at 8 A.M., (b) orthographic top view at 8 A.M.
(c) isometric view at 10 A.M., (d) orthographic top view at 10 A.M.
(e) isometric view at 12 P.M., (f) orthographic top view at 12 P.M. (Continue next page)

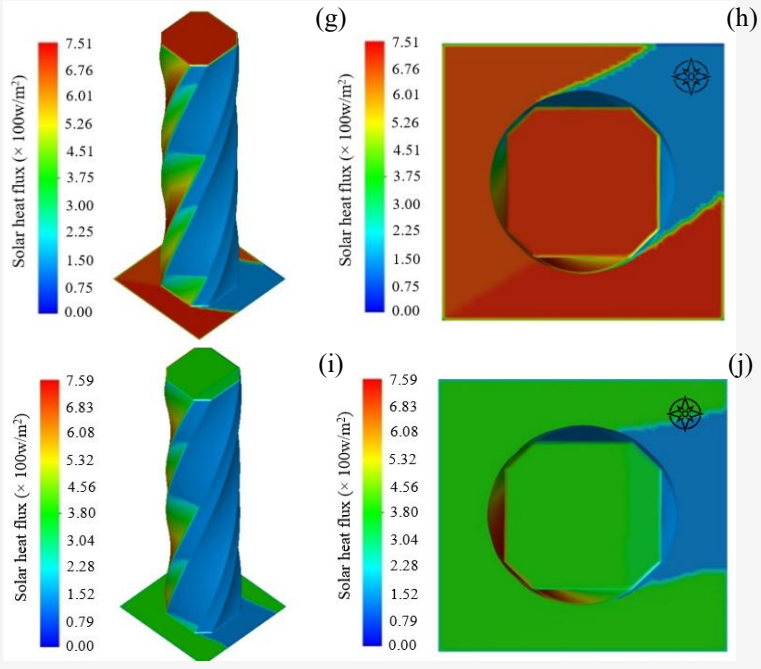

Figure 11: Simulation for March 21st, 2025
(g) isometric view at 2 P.M., (h) orthographic top view at 2 P.M.
(i) isometric view at 4 P.M., (j) orthographic top view at 4 P.M.
(Continue from previous page)

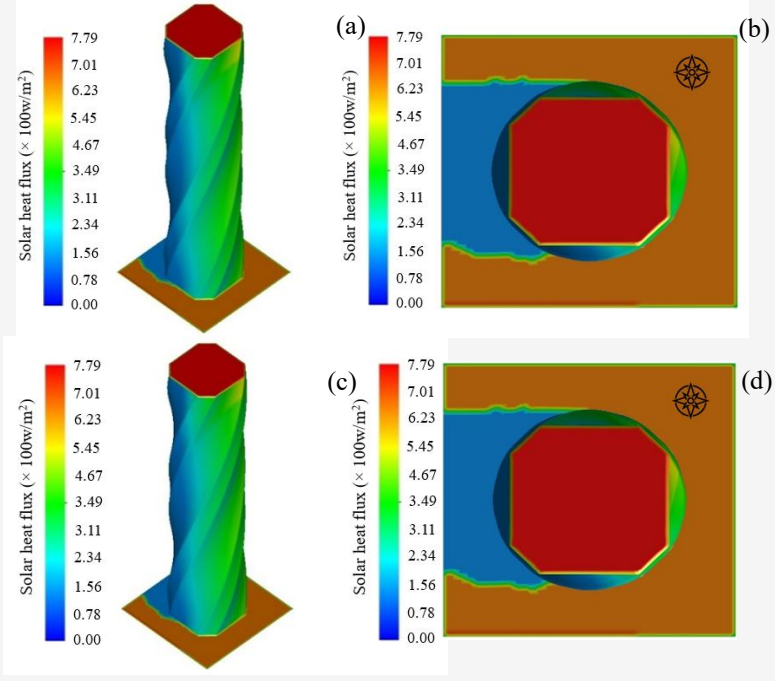

Figure 12: Simulation for June 21st, 2025
(a) isometric view at 8 A.M., (b) orthographic top view at 8 A.M.
(c) isometric view at 10 A.M., (d) orthographic top view at 10 A.M.
(Continue next page)

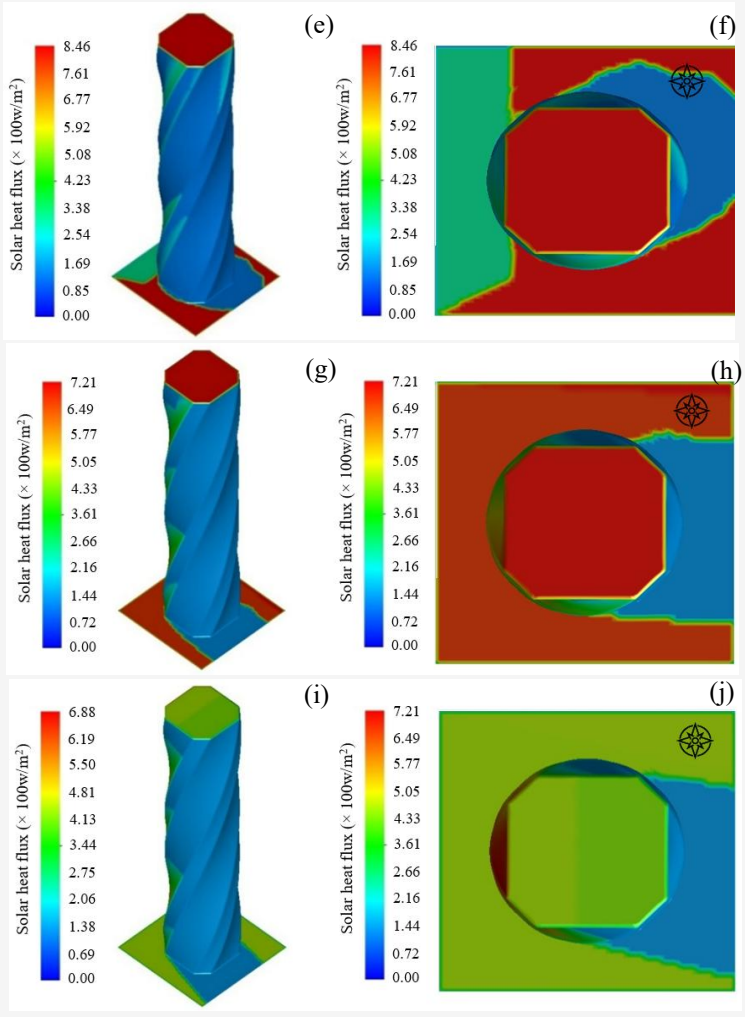

Figure 12: Simulation for June 21st, 2025
(e) isometric view at 12 P.M., (f) orthographic top view at 12 P.M.
(g) isometric view at 2 P.M., (h) orthographic top view at 2 P.M.
(i) isometric view at 4 P.M., (j) orthographic top view at 4 P.M.
(Continue from previous page)

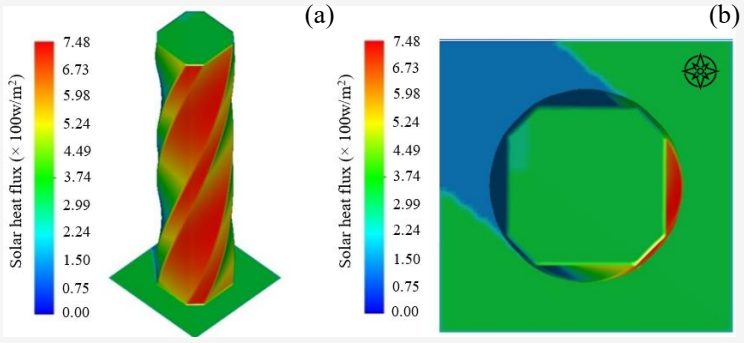

Figure 13: Simulation for winter solstice- Dec 21st, 2025
(a) isometric view at 8 A.M., (b) orthographic top view at 8 A.M.
(Continue next page)

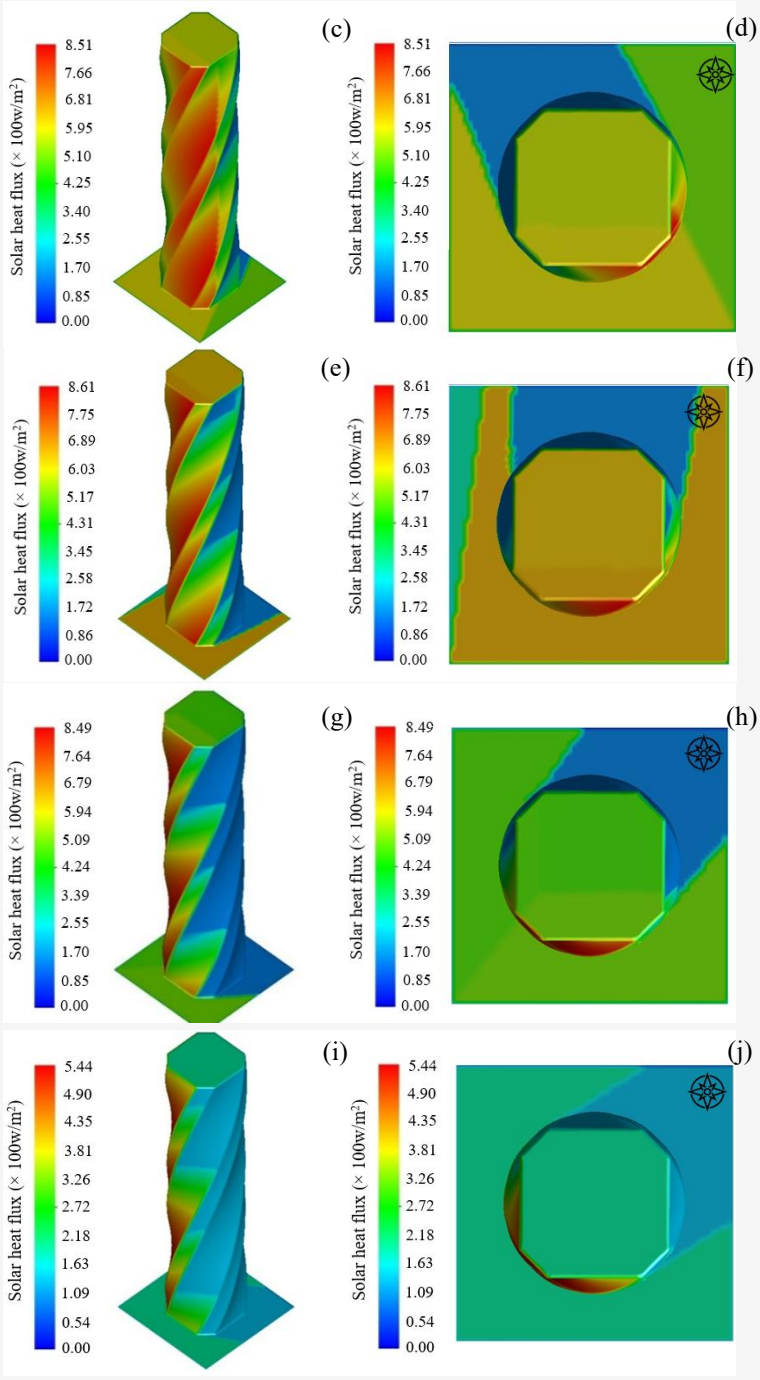

Figure 12: Simulation for June 21st, 2025
(c) isometric view at 10 A.M., (d) orthographic top view at 10 A.M.
(e) isometric view at 12 P.M., (f) orthographic top view at 12 P.M.
(g) isometric view at 2 P.M., (h) orthographic top view at 2 P.M.
(i) isometric view at 4 P.M., (j) orthographic top view at 4 P.M.
(Continue from previous page)

The analysis shows east, and west facades effectively capture solar energy during peak hours, while north-facing ones receive minimal sunlight. Summer offers higher solar intensity and longer daylight, though winter still allows east and west facades to harness energy. South-facing facades gain valuable sunlight

in December. Optimizing solar systems requires leveraging these favorable orientations for maximum efficiency. The analysis shows how building orientation affects solar energy potential, emphasizing optimal radiation capture from morning to evening. Aligning with the Sun's path throughout the year - summer, winter, or equinox - maximizes solar gains, making orientation a key factor in sustainable building design.

7. Empirical Solar Analysis for Validation

Empirical solar models are mathematical frameworks used to estimate solar radiation based on observable meteorological factors. These models utilize historical data to create correlations that predict solar energy availability at specific locations. The significance of these models lies in their ability to provide reliable estimates of solar radiation, aiding in the design and optimization of solar energy systems. This predictive capability is essential for advancing renewable energy projects and facilitating informed decision-making in solar technology deployment.

Four empirical models namely Ghouard, Perrin-Brichambaut, Capderou, and Bird and Hulstrom were compared for predicting daily direct, diffuse, and global solar radiation intensities. Ghouard's model was noted for its superior accuracy in clear skies in Tetuan, Morocco, outperforming the others. BNC Publishing. BNC Publishing [28]. Various models was evaluated to estimate solar radiation, using statistical parameters like mean bias error and root mean square error. The analysis identified the Ghouard's model and Campbell model as the top performers for instantaneous, daily, and monthly estimations, respectively [29]. Multiple models were also assessed and the results found that Ghouard's model to be the most effective, achieving a coefficient of determination above 96.2% [30]. Solar energy potential in Nouakchott, Mauritania, using four models (Link Cloudiness Factor, Perrin-Brichambaut, Ghouard, and Bird Hulstrom) were compared to analyze solar radiation under different sky conditions. The results found that Ghouard's model excelled during the dry season for moderately covered skies [31].

The study of urban solar energy potential in 10 Chinese cities, Ghouard's model was selected for its effectiveness in estimating daily direct irradiation, showcasing its importance for deploying solar energy in urban environments [22]. The article having comparative study among solar Models and Artificial Intelligence approaches for PV Power Forecasting highlights Ghouard's model as integral in enhancing photovoltaic power forecasting through AI, demonstrating improved accuracy compared to traditional methods [27]. A method for estimating solar energy potential in buildings was explored. It advocates for using photogrammetric mesh models alongside Ghouard's model for solar irradiance calculations, emphasizing its role in effective urban planning [32]. Recent advancements in renewable energy systems was reviewed, it emphasized the integration of technologies like AI and IoT [15]. Ghouard's model is highlighted for its predictive accuracy in solar radiation estimation, essential for energy management and planning.

Four models were evaluated for forecasting solar irradiation in Morocco, using satellite data from 2005 to 2020. The results found that Ghouard's model emerged as a top performer with R^2 values reaching 0.97, indicating strong accuracy, while the Bird and Hulstrom model showed poorer results. Ghouard's model is favoured for its ability to calculate daily irradiation based on hourly solar illumination, effectively accounting for variations in solar position throughout the day [33]. The solar irradiance accumulating over time and across various surfaces, represent the total solar energy received by building throughout the day, month, or year. To accurately estimate this solar potential for the building, Ghouard's model that consider astronomical parameters and atmospheric conditions specific to the region is used.

The turbidity factor is essential in atmospheric science, measuring atmospheric clarity and its impact on solar radiation, this research considered normal atmospheric conditions for the estimation of solar potential. Mathematically, turbidity is often defined as a function of aerosol optical depth (AOD), taking into account aerosol scattering and absorption across different wavelengths. Ghouard's model turbidity considered is detailed in Table 3. This model is designed to calculate the solar radiance on the building's walls for each day, allowing for the assessment of its solar energy potential. The hourly global irradiance (E_{global}) for the sunshine duration throughout the year has been calculated for all the building surfaces in the study area and is obtained using Equation 1:

$$E_{global}(h) = E_{direct} + E_{diffuse} \quad \text{Equation 1}$$

Where h is the sunshine hours, E_{direct} is the irradiance directly incident on a face per unit area and can be calculated using Equation 2:

$$E_{direct} = S_0 C_t A_1 \exp\left(-\frac{A_2}{\sin(h_s)}\right)\sin(h_s) \quad \text{Equation 2}$$

C_t is the correction factor for earth-sun distance, which varies from 144 (21 December) to 154 million km (21 June) and can be calculated using Equation 3:

$$C_t = 1 + 0.034\cos(j - 2), \quad j \in [1, 365]$$

Equation 3

j is the day number of the year, ranging from 1 on 1 January to 365 on 31 December

S_0 is the solar constant, which is defined as the energy flux received by a unit area having a value of 1367 W/m^2

A_1 and A_2 are coefficients of the turbidity factor

h_s is the solar elevation in degrees, representing the angle between the horizontal plane with the sun direction, which varies from -90 (nadir) to 0 at sunrise and sunset to -90 (zenith) and is calculated using Equation 4 from the geographical coordinates represented by the latitude ($\varnothing$), solar declination (δ) and altitude hour angle (ω) as shown in Equation 4:

$$\sin(h_s) = \sin\phi\sin\delta + \cos\phi\cos\delta\cos\omega$$

Equation 4

$E_{diffuse}$ is the diffuse irradiance that comes from all the space and has no privileged orientation and is calculated using Equation 5:

$$E_{diffuse} = S_0 C_t \left(0.271 - 0.2939 A_1 \cdot \exp\left(-\frac{A_2}{\cos(h_s)}\right)\right)\cos(h_s)$$

Equation 5

The monthly average daily global horizontal irradiation (GHI) values for the selected building rooftop vary from 3.59 kWh/m²/day in December to 8.21 kWh/m² in June. For the selected building, the average solar irradiation is as presented in Table 4. One significant advantage of the approach used in the research is its capability to simulate the distribution of solar irradiation on building facades, which is crucial for structures with varying orientations and surface characteristics. For the selected building, considered the azimuth of the wall surface, maintaining a tilt angle of 90 degrees for vertical surfaces. This incorporation of variables allows for a more accurate representation of how solar radiation interacts with each facade. The model calculates solar irradiation on an hourly basis during sunshine hours, enabling the estimation of daily, monthly, and yearly average radiation on the building and its envelopes. The model specifically simulates the distribution of solar irradiation by considering the azimuth of building walls while accounting for the tilt angle being 90 degrees for facades and 0 degrees for rooftop. The analysis was conducted across five distinct time intervals, specifically during the days of the equinoxes and the summer and winter solstices. These key dates were selected to capture the variations in solar energy, ensuring a comprehensive representation of incoming solar radiation throughout the year. The Table 5 presents a comparative overview of the solar potential values computed using both ANSYS FLUENT (Method-1) and the Ghouard's Model (Method-2) for each of these critical time intervals.

Table 3: Turbidity factors based on Climatic Conditions [29]

Climatic Conditions	Sky Very Pure	Normal Conditions	Sky Polluted
A_1	0.87	0.88	0.91
A_2	0.17	0.26	0.43

Table 4: Simulated results on selected building rooftop

Building Rooftop (Months)	Estimated Solar Potential Values (kwh/m^2/day)
1	3.86
2	4.83
3	5.47
4	6.54
5	7.55
6	8.21
7	7.79
8	7.51
9	6.86
10	5.78
11	4.5
12	3.59
Total	**72.49**

Table 5: Comparative overview of solar potential on selected building rooftop and facades

Time		08:00		10:00		12:00		14:00		16:00	
Method		1	2	1	2	1	2	1	2	1	2
Rooftop	Jun-21	421.56	418.39	718.25	736.25	780.25	790.89	718.26	709.32	413.96	396.29
	Mar-21	385.21	391.25	670.17	682.14	711.47	723.67	677.62	690.54	326.64	333.86
	Dec-21	284.75	289.24	542.35	538.29	609.58	615.85	418.49	419.62	209.82	211.69
East Façade	Jun-21	690.36	684.26	478.26	490.85	178.23	165.28	144.62	149.49	62.45	58.87
	Mar-21	615.36	621.98	596.23	584.62	242.95	236.95	112.59	108.56	83.26	79.62
	Dec-21	542.29	536.25	455.23	436.26	139.85	132.49	105.36	99.26	83.26	72.67
West Façade	Jun-21	78.63	75.26	142.29	140.59	165.23	158.58	460.45	465.29	619.26	627.98
	Mar-21	56.32	50.84	102.55	99.42	220.98	228.65	315.96	318.95	523.69	519.85
	Dec-21	48.98	46.29	102.63	90.28	145.42	136.24	215.23	212.69	566.27	556.64
South Façade	Jun-21	210.58	212.95	231.25	245.69	186.25	178.63	130.25	142.91	95.36	98.85
	Mar-21	159.25	165.66	389.21	394.54	455.41	438.52	428.23	418.45	278.63	269.64
	Dec-21	234.96	245.29	593.11	597.87	702.32	685.26	652.36	654.29	385.25	379.51
North Façade	Jun-21	158.36	141.35	61.56	59.03	135.24	138.26	127.65	125.31	52.62	49.23
	Mar-21	134.25	109.26	53.69	55.26	122.95	120.59	104.22	96.89	42.98	38.69
	Dec-21	85.84	63.47	44.26	36.95	96.53	89.26	85.84	79.26	38.67	35.95

This allows for a clear understanding of how different methods assess solar energy potential across varying seasonal conditions. The average deviation percentage between Method 1 and Method 2 for the rooftop data is approximately 0.49% The overall average deviation percentage for all four façades is approximately 0.93%. This indicates a general consistency between the two methods across the rooftop and façades analysed.

The solar potential assessment for the rooftop across three critical dates reveals significant variations influenced by seasonal changes. On summer solstice, the highest solar potential was recorded in mid-day, with ANSYS FLUENT (method-1) showing a peak value of 780.25 W/m², while the Ghouard's Model (method-2) noted a close figure of 790.89 W/m². In contrast, the lowest potential was observed on winter solstice, with values dropping to 284.75 W/m² for method-1 and 289.24 W/m² for the method-2. The analysis highlights that solar potential on Rooftop is maximized during the summer months, while winter months demonstrate a considerable decline, emphasizing the impact of seasonal variations on solar energy harvesting capabilities.

The East façade demonstrates the highest solar energy capture, peaking at 690.36 W/m² at 08:00 AM. This is due to its optimal orientation, which allows for maximum exposure to direct sunlight during the early hours of the day. Conversely, the lowest energy capture of 62.45 W/m² occurs at 4 PM, reflecting the diminishing sunlight as the day progresses. June is identified as the best month for energy capture on this façade, benefiting from longer daylight hours and favourable solar angles. The West façade achieves its highest energy capture of 627.98 W/m² at 4 PM, capitalizing on the afternoon sun. This orientation effectively absorbs solar energy as the sun sets, making it a valuable time for energy generation. While it performs well, its overall potential is lower than that of the East facade. The South façade captures a peak energy of 702.2 W/m², indicating its capacity for significant solar energy absorption. December reflects higher values overall; it is the best month for south façade. The maximum energy capture for the North façade was observed June, registering around 158 W/m². However, overall performance is low due to the limited direct sunlight exposure on the North side. Given these findings and the general inefficiency of North-facing solar energy capture in the Northern Hemisphere, it may not be practical to rely on the North façade for significant solar energy extraction using standard PV technologies.

8. Conclusion

The south facade experiences significantly good solar energy exposure during the winter solstice due to the sun's low elevated angle and trajectory. The sunlight strikes the south facade at a more oblique angle, diminishing direct exposure and, consequently, solar potential. The east and west facades exhibit strong solar potential year-round, benefiting from morning and afternoon sunlight, respectively. They effectively capture energy, particularly in the months leading up to and following the summer solstice, making them valuable for solar energy generation and enhancing the overall performance of the rooftop by maximizing exposure throughout the day. These insights highlight the critical role of facade orientation in optimizing solar energy potential in urban environments. Although facade energy production is generally lower than that of rooftops, the contributions from east and west facades, especially during summer months, demonstrate that

vertical surfaces can still capture significant solar energy under favourable conditions. This highlights the importance of surface orientation in green building design, as it enables effective solar energy capture during peak sunlight hours. In conclusion, the 3D spatial analysis conducted on United Tower confirms its significant solar potential, particularly in the east, west, and south orientations. The findings indicate that the building can effectively harness solar energy throughout the year, making it a suitable for the installation of Building-Integrated Photovoltaics (BIPV) technology. This research highlights the tower's capability to contribute to sustainable building practices but also emphasizes the role of innovative architectural designs in promoting renewable energy solutions within urban environments.

Acknowledgement
This research was supported for publication by Bahrain Polytechnic's institutional funding with Ref. number AREC/PUB/2026/010.

References

[1] Alnaser, N. W., Albuflasa, H. M. and Alnaser, W. E., (2022). The Transition in Solar and Wind Energy Use in Gulf Cooperation Council Countries (GCCC). *Renewable Energy and Environmental Sustainability*, Vol. 7(4). https://doi.org/10.1051/rees/2021034.

[2] Belal, G., Saddam Akber Abbasi, S. A. and Muhammad, A., (2023). Application of Solar PV in the Building Sector: Prospects and Barriers in the GCC Region, *Energy Reports,* Vol. 9*,* 3932-3942. https://doi.org/10.1016/j.egyr.2023.02.085.

[3] Salem, H. S., Pudza, M. Y. and Yihdego, Y., (2023). Harnessing the Energy Transition from Total Dependence on Fossil to Renewable Energy in the Arabian Gulf Region, Considering Population, Climate Change Impacts, Ecological and Carbon Footprints, and United Nations' Sustainable Development Goals. *Sustainable Earth Reviews*, Vol. 6(1). https://doi.org/10.1186/s42055-023-00057-4.

[4] Al-Saidi, M., (2022). Disentangling the SDGs agenda in the GCC region: Priority Targets and Core Areas for Environmental Action. *Frontiers in Environmental Science*, Vol. 10. https://doi.org/10.3389/fenvs.2022.1025337.

[5] Pereira, M. C. R. and Coria, A. S., (2022). Environmental Impacts of Solar Photovoltaic Systems: A Revision from Life Cycle Assessments and Other Studies. *Revista EIA*, Vol. 19(38), 1-8. https://doi.org/10.24050/reia.v19i38.1570.

[6] Bandara, S. B. G. M., Fernando, H. H. D., Herath, H. M. P. Y. C. B., Nayomi, M. D. R., Samaranayake, B. G. L. T., Ekanayake, J. B. and Mohotti, A. J., (2025). Optimizing Agro-Voltaic Systems: Enhancing Agricultural Productivity and Energy Generation through Transparent Solar Arrays. *Ceylon Journal of Science*, Vol. 54(1), 233–238. https://doi.org/10.4038/cjs.v54i1.8497.

[7] EzzEldin, A. A., Alnaser, N. W., Flanagan., R. and Alnaser, W. E., (2022). The Feasibility of using Rooftop Solar PV Fed to the Grid for Khalifa Town Houses in the Kingdom of Bahrain, *Energy and Buildings,* Vol. 276. https://doi.org/10.1016/j.enbuild.2022.112489.

[8] Chen, L., Hu, Y., Wang, R., Li, X., Chen, Z., Hua, J., Osman, A. I., Farghali, M., Huang, L., Li, J., Dong, L., Rooney, D. W. and Yap, P. S., (2024). Green Building Practices to Integrate Renewable Energy in the Construction Sector: A Review. *Environmental Chemistry Letters*, Vol. 22(2), 751–784. https://doi.org/10.1007/s10311-023-01675-2.

[9] Etukudoh, E. A., Nwokediegwu, Z. Q. S., Umoh, A. A., Ibekwe, K. I., Valentine Ikenna Ilojianya, V. I. and Adefemi, A., (2024). Solar Power Integration in Urban Areas: A Review of Design Innovations and Efficiency Enhancements. *World Journal of Advanced Research and Reviews*, Vol. 21(1), 1383–1394. https://doi.org/10.30574/wjarr.2024.21.1.0168.

[10] Wongwan, W., Pleerux, N., Thanomsat, N., and Moukomla, S. (2024). Technical and Economic Potential of Solar Energy on Rooftops: A Case Study at Lampang Rajabhat University, Thailand. *International Journal of Geoinformatics*, Vol. 20(2), 82–94. https://doi.org/10.52939/ijg.v20i2.3069.

[11] Vijayan, D. S., Koda, E., Sivasuriyan, A., Winkler, J., Devarajan, P., Kumar, R. S., Jakimiuk, A., Osinski, P., Podlasek, A. and Vaverková, M. D., (2023). Advancements in Solar Panel Technology in Civil Engineering for Revolutionizing Renewable Energy Solutions-A Review. *Energies*, Vol. 16(18). https://doi.org/10.3390/en16186579.

[12] Liu, H. Y., Skandalos, N., Braslina, L., Kapsalis, V. and Karamanis, D., (2023). Integrating Solar Energy and Nature-Based Solutions for Climate-Neutral Urban Environments. *Solar*, Vol. 3(3), 382–415. https://doi.org/10.3390/solar3030022.

[13] Akpan, J. and Olanrewaju, O., (2023). Sustainable Energy Development: History and Recent Advances. *Energies*, Vol. 16(20). https://doi.org/10.3390/en16207049.

[14] Lai, C. M. and Hokoi, S., (2015). Solar Façades: A review. *Building and Environment*, Vol. 91, 152–165. https://doi.org/10.1016/j.buildenv.2015.01.007.

[15] Khare, V., Khare, C., Nema, S. and Baredar, P., (2021(a)). Renewable Energy System Paradigm Change from Trending Technology: A Review. *International Journal of Sustainable Energy*, Vol. 40(7), 697–718. https://doi.org/10.1080/14786451.2020.1860043.

[16] Polo, J., Martín-Chivelet, N., Alonso-Abella, M. and Alonso-García, C., (2021). Photovoltaic Generation on Vertical Façades in Urban Context from Open Satellite-Derived Solar Resource Data. *Solar Energy*, Vol. 224, 1396–1405. https://doi.org/10.1016/j.solener.2021.07.011.

[17] Putra, I. D. G. A., Nimiya, H., Kubota, T., Lee, H. S., Iketani, F., Trihamdani, A. R., Sopaheluwakan, A., Alfata, M. N. F., Permana, D. S. and Pradana, R. P., (2023). Study of Vertical Solar Irradiance and Local Scale Climate to Assess Passive Cooling Potential in Tangerang of Indonesia. *E3S Web of Conferences*, Vol. 396. https://doi.org/10.1051/e3sconf/202339605002

[18] Zhao, K. and Gou, Z., (2023). Influence of Urban Morphology on Facade Solar Potential in Mixed-Use Neighborhoods: Block Prototypes and Design Benchmark. *Energy and Buildings*, Vol. 297. https://doi.org/10.1016/j.enbuild.2023.113446.

[19] Elmalky, A. M. and Araji, M. T., (2023). Computational Procedure of Solar Irradiation: A New Approach for High Performance Façades with Experimental Validation. *Energy and Buildings*, Vol. 298. https://doi.org/10.1016/j.enbuild.2023.113491.

[20] Liang, H., Shen, J., Yip, H. L., Fang, M. M. and Dong, L., (2024). Unleashing the Green Potential: Assessing Hong Kong's Building Solar PV Capacity. *Applied Energy*, Vol. 369. https://doi.org/10.1016/j.apenergy.2024.123567.

[21] Ryali, N. S. D., Tripathi, N. K., Ninsawat, S. and Singh, J. G., (2024). Geospatial Assessment of Solar Energy Potential: Utilizing MATLAB and UAV-Derived Datasets. *Buildings*, Vol. 14(6). https://doi.org/10.3390/buildings14061781.

[22] Velastegui-Montoya, A., Montalván-Burbano, N., Carrión-Mero, P., Rivera-Torres, H., Sadeck, L. and Adami, M., (2023). Google Earth Engine: A Global Analysis and Future Trends. *Remote Sensing*, Vol. 15(14). https://doi.org/10.3390/rs15143675.

[23] Kumar, L. and Mutanga, O., (2018). Google Earth Engine Applications Since Inception: Usage, Trends, and Potential. *Remote Sensing*, Vol. 10(10). https://doi.org/10.3390/rs10101509.

[24] Lalaeng, S., Thanasang, T., Puttinet, P., Srireuan, N., and Chavanavesskul, S. (2024). The Relationship between PM2.5 and Solar Cell Electricity Generation Using Aerosol Optical Depth (AOD). *International Journal of Geoinformatics*, Vol. 21(1), 83–96. https://doi.org/10.52939/ijg.v21i1.3797.

[25] Bhor, D., Pote, R. T., Chavan, N. and Pote, R., (2022). Comparative Thermal Analysis of Different Solar Panel Materials using ANSYS; Comparative Thermal Analysis of Different Solar Panel Materials using ANSYS. *International Journal of Engineering Research*, Vol. 16(6). https://doi.org/10.5281/zenodo.18439878.

[26] Harsito, C., Triyono, T. and Rovianto, E., (2022). Analysis of Heat Potential in Solar Panels for Thermoelectric Generators using ANSYS Software. *Civil Engineering Journal (Iran)*, Vol. 8(7), 1328–1338. https://doi.org/10.28991/CEJ-2022-08-07-02

[27] Ben Ammar, R., Ben Ammar, M. and Oualha, A., (2021). Comparative Study among Physical Models and Artificial Intelligence Methods for PV Power Forecasting. *18th IEEE International Multi-Conference on Systems, Signals and Devices, SSD 2021*, 1038–1046. https://doi.org/10.1109/SSD52085.2021.9429452.

[28] El Mghouchi, Y., Ajzoul, T., Taoukil, D. and El Bouardi, A., (2016). The Most Suitable Prediction Model of the Solar Intensity, on Horizontal Plane, at Various Weather Conditions in a Specified Location in Morocco. *Renewable and Sustainable Energy Reviews*, Vol. 54, 84–98. https://doi.org/10.1016/j.rser.2015.09.089.

[29] El Mghouchi, Y., El Bouardi, A., Choulli, Z. and Ajzoul, T., (2016). Models for Obtaining the Daily Direct, Diffuse and Global Solar Radiations. *Renewable and Sustainable Energy Reviews*, Vol. 56, 87–99. https://doi.org/10.1016/j.rser.2015.11.044.

[30] Sidibba, A., Ndiaye, D., Bouhamady, S. and El Bah, M., (2019). Characterization and Modeling of Solar Radiation on the Ground, Application to the Estimate of Solar Potential Available on the Coast of Nouakchott. *OAJ Materials and Devices*, Vol. 4(1). https://doi.org/10.23647/ca.md20191702.

[31] Jiddou ABDI, E., Mahmoud ALI, M., Bilal, B., Dia, N., Ndongo, M., Mohamed Fadel KEBE, C. and Alioune NDIAYE, P., (2019). Seasonal Analyses of Solar Radiation on Flat Ground for Different State of Sky: Case of Nouakchott, Mauritania. *International Journal of Physical Sciences Full Length Research Paper*, Vol. 14(12), 125–138. https://doi.org/10.5897/IJPS2019.4830.

[32] Zhang, Y., Dai, Z., Wang, W., Li, X., Chen, S. and Chen, L., (2021). Estimation of the Potential Achievable Solar Energy of the Buildings Using Photogrammetric Mesh Models. *Remote Sensing,* Vol. 13(13). https://doi.org/10.3390/rs13132484.

[33] Halima, Y., Youness, E. M. and Abdeljabar, K., (2022). Performance Assessment of Solar Radiation Based on Satellite Data in a Moroccan City. *2022 International Conference on Data Analytics for Business and Industry, ICDABI 2022*, 533–537. https://doi.org/10.1109/ICDABI56818.2022.10041258.